Journal of Structural Biology 215 (2023) 108030

Contents lists available at ScienceDirect

Journal of Structural Biology

journal homepage: www.elsevier.com/locate/yjsbi

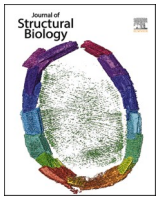

Research Article

Local defocus estimation in single particle analysis in cryo-electron microscopy

E. Fernandez-Gimenez [a,b], J.M. Carazo [a], C.O.S. Sorzano [a,*]

[a] Centro Nac. Biotecnologia (CSIC), c/Darwin, 3, 28049 Cantoblanco, Madrid, Spain
[b] Univ. Autonoma de Madrid, 28049 Cantoblanco, Madrid, Spain

ARTICLE INFO

Keywords:
Local defocus
Defocus
CTF
High-resolution
SPA
Cryo-EM

ABSTRACT

Single Particle analysis (SPA) aims to determine the three-dimensional structure of proteins and macromolecular complexes. The current state of the art has allowed us to achieve near-atomic and even atomic resolutions. To obtain high-resolution structures, a set of well-defined image processing steps is required. A critical one is the estimation of the Contrast Transfer Function (CTF), which considers the sample defocus and aberrations of the microscope. Defocus is usually globally estimated; in this case, it is the same for all the particles in each micrograph. But proteins are ice-embedded at different heights, suggesting that defocus should be measured in a local (per particle) manner. There are four state-of-the-art programs to estimate local defocus (Gctf, Relion, CryoSPARC, and Xmipp). In this work, we have compared the results of these software packages to check whether the resolution improves. We have used the Scipion framework and developed a specific program to analyze local defocus. The results produced by different programs do not show a clear consensus using the current test datasets in this study.

1. Introduction

Single Particle Analysis (SPA) by cryo-electron microscopy (cryo-EM) has become an established field to elucidate the atomic model of macro-molecules and biological complexes, as it can obtain high-resolution (below 3 Å) Coulomb potential maps. Achieving good resolution maps is becoming easier using state-of-the-art methods(Neumann et al., 2018; Vilas et al., 2022). However, to obtain high resolution, details matter. One of the best-known sources of issues in cryo-EM is the proper correction of the contrast transfer function (CTF) (Sorzano et al., 2021b).

Out-of-focus image acquisition, i.e., defocus, is the main phase contrast mechanism in cryo-EM (Danev et al., 2020). A good CTF estimation allows for correcting aberrations and defoci, as CTF is affected by these acquiring conditions. Thus, this function must be determined for each micrograph during its processing. CTF estimation and correction is one of the first steps in the general workflow used in SPA. However, this is usually done in a global approach, as the CTF is estimated and corrected for the whole micrograph, i.e., each particle of the same micrograph has the same CTF correction.

Nevertheless, it is known that a more precise CTF correction could be done by refining the global estimation for each particle, called local CTF estimation or refinement. In this way, based on the global CTF determination for each micrograph, some methods estimate the local CTF correction for each particle that appears in that micrograph. In this study, we are specifically interested in the local defocus estimation.

The local defocus refinement step is important when one wants to improve resolution once the map is already at high resolution (or close to it), as the sample has a certain thickness and the macro-molecules in it have been frozen at different heights inside the ice layer(Noble et al., 2018) (see Fig. 1). This causes small differences in each particle's defocus value, even though they are in the same micrograph. Still, these differences are big enough to cause blurring if the same defocus is used for all particles in the same micrograph. There are several state-of-the-art methods that perform local defocus estimation, such as Gctf (Zhang, 2016), Relion(Zivanov et al., 2020), CryoSPARC(Punjani and Fleet, 2020), and Xmipp(Strelak et al., 2021; de la Rosa-Trevin et al., 2013; Sorzano et al., 2004).

All these packages estimate the local defocus, and in this work, we try to estimate how precise those estimations are. As we cannot compare the different estimations versus the (unknown) ground truth, we have performed a comparative study between the results of the four state-of-

* Corresponding author.
E-mail address: coss@cnb.csic.es (C.O.S. Sorzano).

https://doi.org/10.1016/j.jsb.2023.108030
Received 1 July 2023; Received in revised form 30 August 2023; Accepted 21 September 2023
Available online 25 September 2023

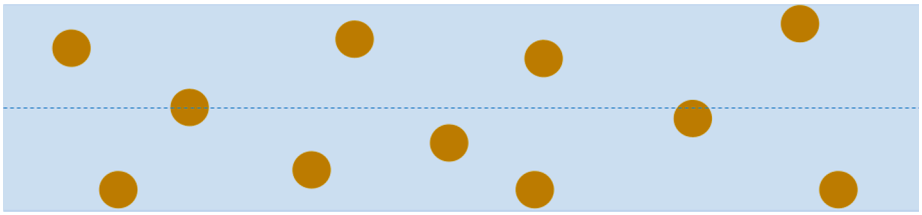

Fig. 1. Distribution of proteins along the ice thickness of the sample(Noble et al., 2018). The dotted line represents the global defocus estimation for the micrograph. However, the height of each particle (schematically represented by yellow dots) in the sample does not agree in many cases with the height corresponding to the global defocus.

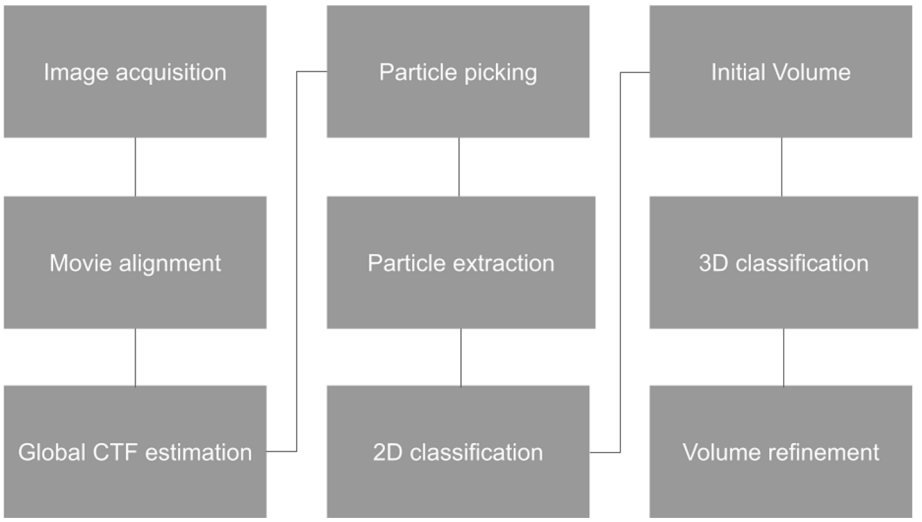

Fig. 2. Standard single particle analysis (SPA) workflow.

the-art methods mentioned before. We aim to know how similar these estimations are between them and corroborate if it is true that local estimations are precise enough to improve resolution, as this is a final step that is performed only in some specific workflows where the user wants to push forward the resolution after refinement and it is difficult to validate.

2. Methods

To perform the comparative study on local defocus estimation, we use Scipion (Jimenez-Moreno et al., 2021; de la Rosa-Trevin et al., 2016) since it is a general framework for cryo-EM image processing that allows the combination and compatibility of different cryo-EM software packages. This simplifies the comparison of results and their interpretation. Thus, we have performed a conventional SPA workflow from movies to final refined volumes. Then, we have included and focused on the different state-of-the-art methods to estimate local defocus (Gctf, Relion, CryoSPARC, and Xmipp).

2.1. Data

The data for this study is an apoferritin sample acquired with a 300 kV CryoArm microscope and a K3 camera at the Spanish National Center for Biotechnology (CNB) Cryo-EM Facility, initially used to check the microscope setting and performance. It consists of 8,721 movies with a pixel size of 0.23Å/pixel, leading to 7,815 micrographs (leaving some of the movies out due to excessive motion blur). Apoferritin has a diameter of approximately 12 nm, and the thickness of the ice in this sample is

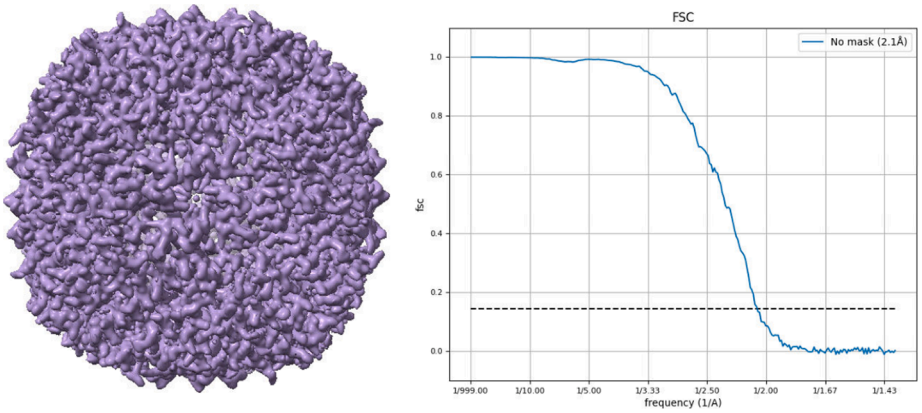

Fig. 3. Final density map for the apoferritin refined with CryoSPARC (considering global defocus estimation) and reported Fourier Shell Correlation (FSC).

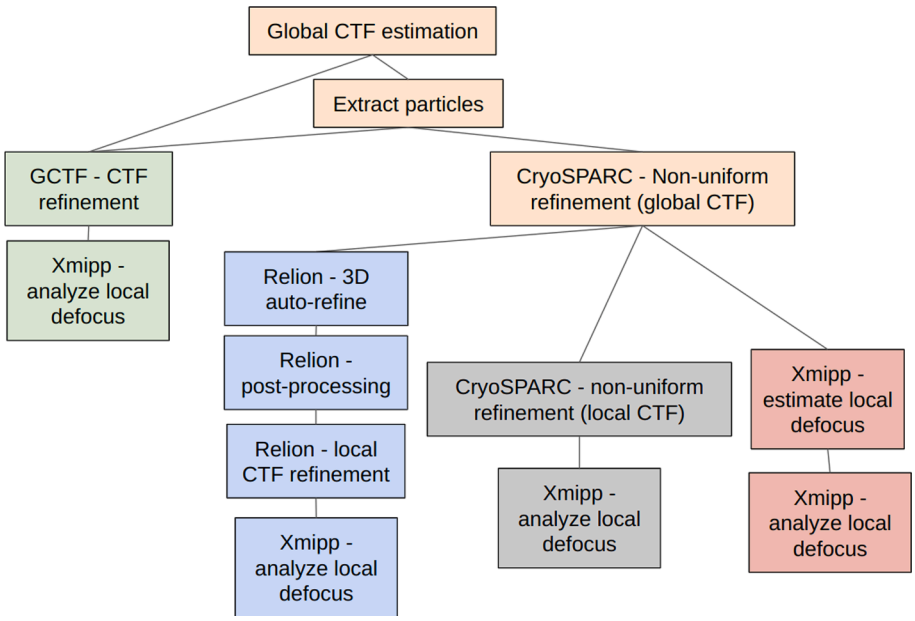

Fig. 4. Local defocus workflow in Scipion developed for this study, including the proposed analysis protocol.

approximately 40 nm, which leaves enough space for the sample to be placed at different heights (defocus) in the thickness of the sample. Apoferritin has been deeply studied in cryoEM (Yip et al., 2020), and it is known to be a very stable protein with high-order symmetry that allows high resolution with standard SPA processing. An in–house acquisition has been chosen instead of a data set coming from a public database to have all the acquisition information and intermediate steps along the processing. This procedure gives us more flexibility to execute the different defocus estimation algorithms at different workflow points.

2.2. Workflow

A common SPA workflow was carried out at the Instruct Image Processing Center (I2PC), combining different software packages in Scipion. The main steps followed in the workflow are listed below, and a standard SPA workflow is summarized in Fig. 2:

1. Movie alignment using MotionCor2 (Zheng et al., 2017).
2. CTF estimation using Gctf (Zhang, 2016).
3. Particle picking with Cryolo(Wagner et al., 2019) and Gautomatch.
4. Extraction of downsampled particles with Relion (Zivanov et al., 2020).
5. Building of initial model with CryoSPARC(Punjani et al., 2017).
6. Several iterative steps of 2-dimensional classification with CryoSPARC to discard bad particles.
7. Re-extraction of original size particles with Xmipp (Strelak et al., 2021; de la Rosa-Trevin et al., 2013; Sorzano et al., 2004).
8. Several iterative steps of CryoSPARC non-uniform refinement(Punjani et al., 2017) with initial model and re-extracted original size particles as input, with global CTF refinement and global beam tilt refinement but no local defocus refinement, achieving a map resolution of 2.1Å as shown in Fig. 3.

Once a refined reconstruction is obtained, we tried to push forward the reconstruction quality by performing a local defocus estimation and correction. To do that, different algorithms were used.

Firstly, we include “Gctf - ctf refinement” after the re-extraction of particles at their original size. This algorithm needs as input the set of particles without alignment, the set of micrographs, and the corresponding set of global CTF estimations. Note that to use the “Gctf - ctf refinement” program, we had to use an older version of Gctf (v. 1.06), as the current one (v. 1.18) does not support local CTF refinement anymore.

As for the defocus refinement algorithms of Relion (v.3.0.0), CryoSPARC (v.4.0.7), and Xmipp (v.22.4.0), they all make use of the same kind of input: the aligned set of particles and a refined reference volume. Note that to perform CryoSPARC defocus refinement, we can carry out the whole non-uniform refinement program because it is one of its options or we can run it as a separate step after the refinement (obtaining practically identical results in both cases). In the case of Relion, there is a specific program to run CTF refinement. However, it needs as input the output of the Relion post-processing program, which in turn needs as input the output of Relion auto-refine (which needs as input the set of particles and a reference volume). In both cases, these complex specificities occur because we are using these different programs outside of their standard workflows, and it makes clear the point that mixing different software suites is not easy; however, Scipion can bridge these issues easily. Finally, Xmipp has a dedicated program to compute CTF refinement, taking as input directly the particles and volume out from any refinement program. Fig. 4 shows the workflow for all the local defocus estimation software tested in this work.

2.3. Xmipp algorithm for Local Defocus Estimation

Each software suite uses different procedures to obtain the local defocus estimation. In this section, we describe how it is done by the algorithm inside the software suite that we develop in our laboratory, that is, Xmipp. Xmipp estimation of local defocus consists of several steps that begin with the computation of the projection of the reference volume corresponding to the alignment of each input particle. Then, the global defocus estimated previously is applied to the corresponding projection of every particle. After that, the correlation between the input particle and the corresponding projection is computed. Finally, the global defocus estimation is refined using the Powell optimization method to look for a local minimum that better matches the particle and the corresponding projection as measured by the correlation. These steps are executed for each input particle. The method is stand-alone to refine local defocus for a set of aligned particles and their refined volume (as used in this study). Still, it is also used in the refinement algorithm HighRes(Sorzano et al., 2018) when the “optimize defocus” option is selected.

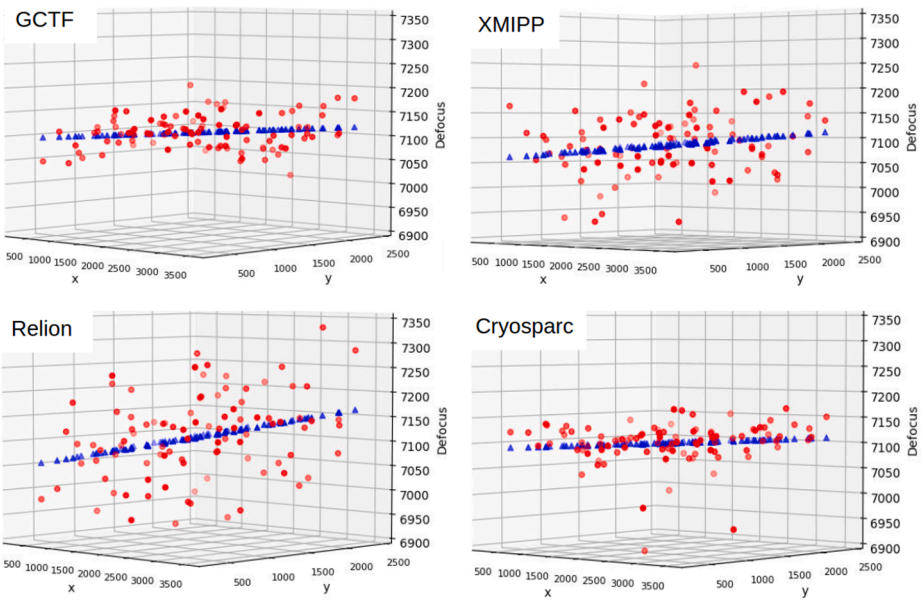

Fig. 5. Plots computed by our analysis protocol of the distribution of all the particles in red (coordinates X and Y are the positions of the particle in the micrograph, while Z coordinate corresponds to the local defocus estimated for the particle in Å) along the thickness of the sample for a particular micrograph of the data set according to the different local defocus estimation software. Note that small differences in the rotation of the axes in each subplot have been made for convenience to better visualize the adjustment plane (blue) in each case.

2.4. Local defocus estimation analysis

To compare different local defocus estimations, we have developed a Scipion protocol that analyses the output of any local defocus estimation software. This protocol uses a least-squares approach to compute a linear fitting (a plane) according to Eq. 1 from the set of local defocus estimations of the particles in each micrograph.

$$\Delta f_i \approx \widehat{\Delta f}_i = \Delta f_0 + a y_i + b x_i, \tag{1}$$

where Δf_0 is the global defocus, Δf_i the local defocus of the i-th particle, and (x_i, y_i) its position in the micrograph. The result is a plot per micrograph of the three-dimensional distribution of the particles in each micrograph, that is, the $(x_i, y_i, \Delta f_i)$ points. The three-dimensional position of each particle in the micrograph and the computed fitting plane are plotted. Thus, this plot approximates the distribution of heights of particles inside the ice and informs about the local defocus estimated variations of the particles in the micrograph.

3. Results and discussion

Section 3.1 shows quantitative differences between the local defocus estimations computed by the different state-of-the-art methods (Gctf, Relion, CryoSPARC, and Xmipp). As the reader will notice, there are perceptible differences, thus, in Section 3.2, we try to elucidate which estimations are reliable.

3.1. Differences between estimations by different software

To better illustrate that the different software programs estimate different local defocus for each particle, we have chosen one representative micrograph of the data set. We show in Fig. 5 the plot produced by our analysis protocol for the same micrograph with the different local

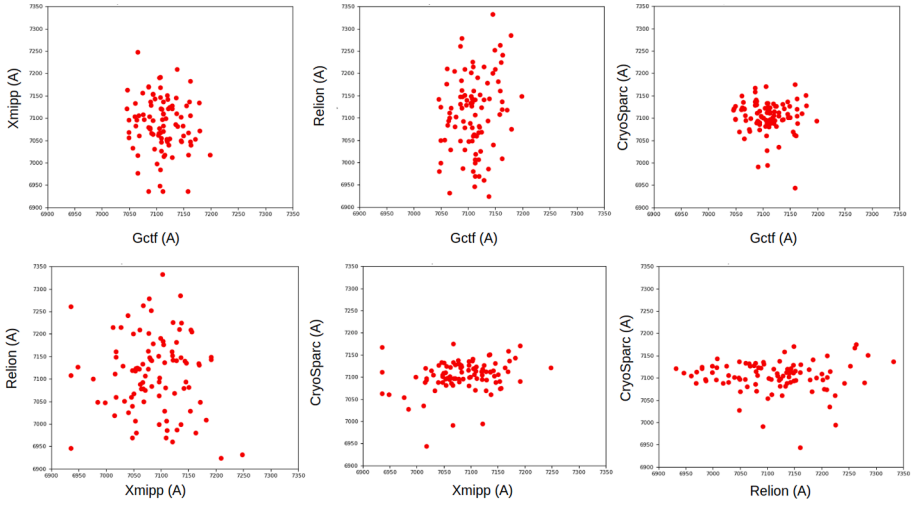

Fig. 6. Scatter plots comparing the local defocus estimations (in Å) of each method versus the others for particles in a selected micrograph of the data set to see how they correlate (perfect correlation would be a diagonal line).

Table 1
Average correlation matrix between the local estimations by the different software and global estimation. The major correlation between methods is in bold.

	Gctf	Relion	Xmipp	CryoSPARC	Global
Gctf	1				
Relion	0.12	1			
Xmipp	0.17	0.12	1		
CryoSPARC	0.26	0.15	**0.40**	1	
Global	0.04	0.25	0.04	0.04	1

defocus estimations. Remarkably, the shape of the defocus distribution of particles in the same micrograph differs according to each method (both the adjusted plane and the distribution around it). It is true that if we consider the dispersion range, the differences are small, meaning that the estimations of the different programs are not very far away. However, as this is considered a refinement step to push forward resolution once the density map is already in high resolution, this result may question the accuracy of the different methods.

To show and compare the differences between the results of the different methods with this chosen example micrograph, we have computed a pair-wise scatter plot of the estimations of the different methods to see how they correlate. Scatter plots are shown in Fig. 6. Note that for total correlation, a diagonal line should appear in the plot; thus, from Fig. 6, we can state that the different methods do not agree. Moreover, their different estimates are completely independent of each other, that is, what one would expect from a random estimation.

To quantify these differences, we have computed the correlation matrix between all the methods for each micrograph. Then, we averaged all matrices, obtaining the average correlation matrix shown in Table 1. Note that we cannot directly compute the correlation matrix of the particles in all micrographs, as the global defocus for each micrograph is different (as they have been acquired at different defocus on purpose). As can be seen from the average correlation matrix, in this particular data set, the major agreement between methods is between CryoSPARC and Xmipp (but note that it is not even 0.5), and the worst is between Gctf and Relion. However, this fact may not be extrapolated to any other data set.

3.2. *Which local defocus estimation should we trust?*

From the previous section, we have shown that local defoci estimations by different software have considerable differences. Unfortunately, the ground truth about local defoci is unknown, so we cannot be sure if any or none of the different estimates are correct. Thus, we have tried to evaluate the quality of each estimation separately.

Firstly, we have computed the scatter plots of each estimation versus the global for the same subset of random particles, shown in the Supplementary material Fig. S-1. Note that in this plot, the range is much bigger as they consider the defocus of every micrograph (and usually, in image acquisition, micrographs are acquired at different defocus on purpose). Thus, we can see that all the estimations correlate fairly well with the global estimation, as expected, meaning that none of them is completely erroneous, as a local defocus estimation may vary from the global, but less than half of the ice thickness (if the variation is bigger, it would mean that the particle is out of the sample, which obviously would be an erroneous estimation).

Afterward, we checked the stability of the methods, as differences in local defoci are small and can be highly affected by noise in the computations. Thus, we have executed two times each local defocus estimation program for particles in the example micrograph used before, and we have computed the scatter plot of each pair of executions to see the correlation. The plots are shown in Fig. 7.

To avoid identical inputs, we have performed two different CryoSPARC non-uniform refinements with the same input particles and reference volume and the same parameters: symmetry, filter type, global CTF refinement parameters (as minimum resolution, global beam tilt refinement, and spherical aberration). Note that refinement is not 100% stable and thus, angles and shifts may slightly vary from one execution to another even with the same parameters(Sorzano et al., 2021a). The outputs of these two refinements have been used separately with each of the local defocus estimation methods (except for Gctf, due to it requiring other inputs). In summary, we have repeated the workflow in Fig. 4 from "CryoSPARC - Non-uniform refinement (global CTF)" to the end.

In the case of Gctf, which uses as input a set of non-aligned particles (i.e., directly from the extraction step), to avoid identical input, we have

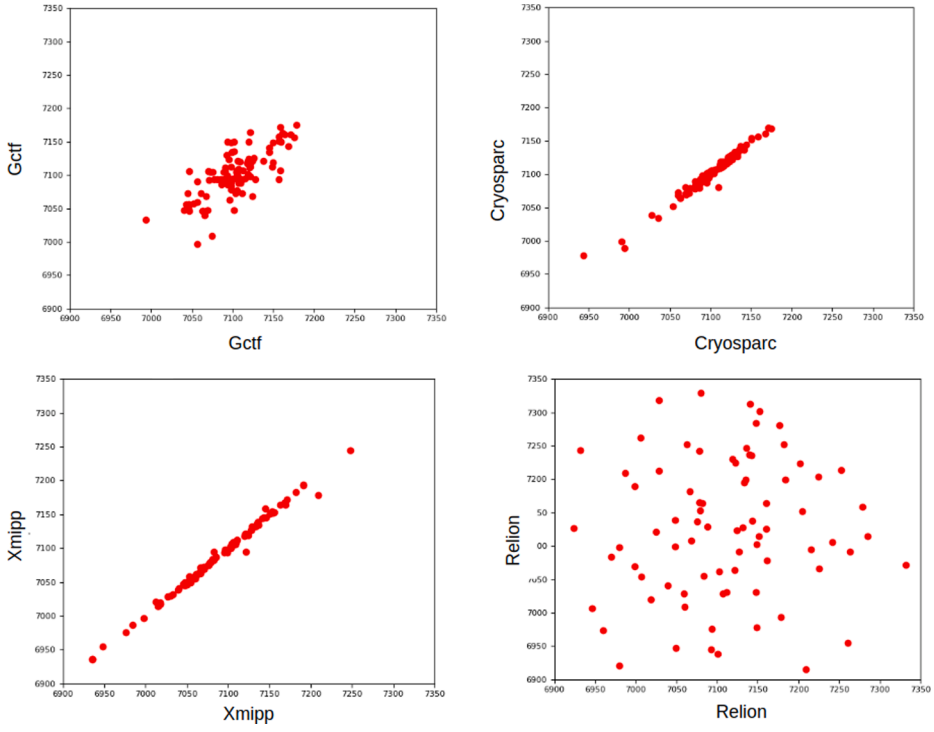

Fig. 7. Scatter plots comparing two executions of each local defocus estimation method for a specific micrograph of the data set to evaluate their stability.

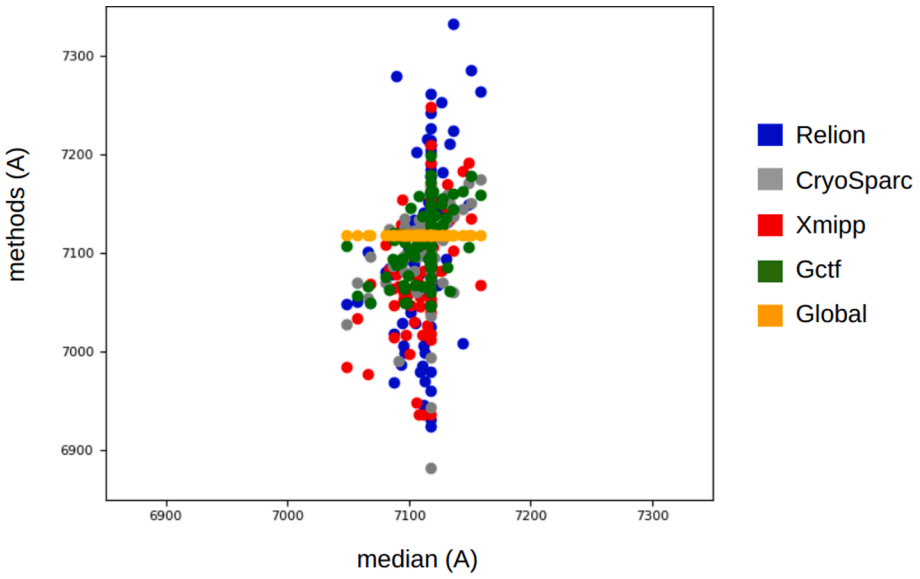

Fig. 8. Scatter plot comparing the median local defocus estimation (in Å) with each local defocus estimation method (in different colors) for all the particles in the chosen example micrograph to see how they correlate and how the different estimations spread around the unknown ground truth.

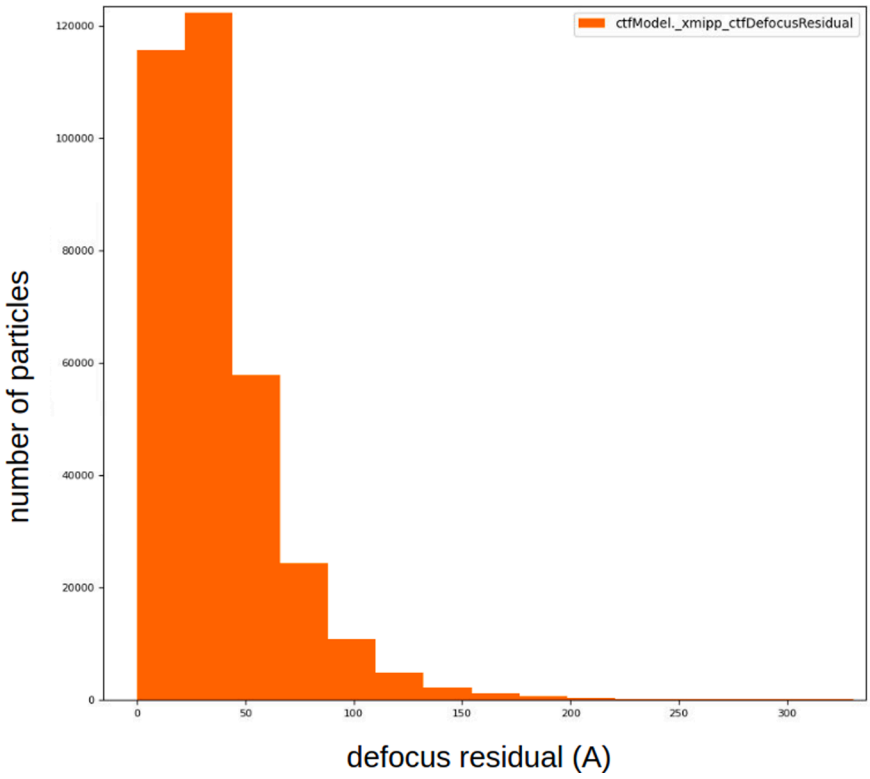

Fig. 9. Histogram of the residuals (computed as the median absolute deviation, MAD) between the median of all local defocus estimations and the original global estimation for each particle.

slightly modified the X and Y coordinates of the input particles by moving them the equivalent of half the size of the protein (i.e., as if particles have been picked off-center). As can be appreciated in Fig. 7, in this case, CryoSPARC and Xmipp are more stable than Gctf and Relion.

As discussed above, we cannot know if a local defocus estimation is correct. We can check if some estimation is too far from the original global one, which would be a clue for an incorrect estimation. We can also check its stability as a measure of reliability. Although some methods are (at least in this case) more stable than others, the differences in the results of different executions are indeed too small to be a reason to fully discard an estimation method (but one must be aware of this instability).

We can compare their estimations to see if they agree, which is not proof of correctness. But if two results computed by two different methods agree makes one think that it is more likely that the solution is correct, as suggested in Sorzano et al. (2021a). Thus, by comparing estimations, we can check that they are close enough not to be able to discard any, and we can also check that the result seems correct for the

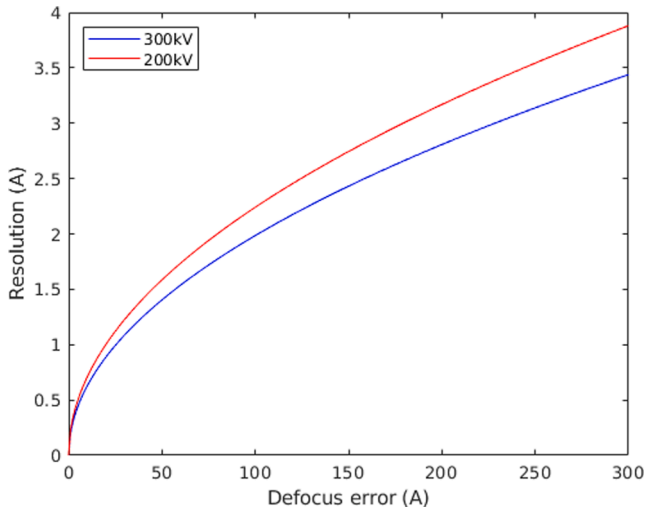

Fig. 10. Resolution limit, $|\mathbf{R}|^{-1}$, with different defocus error for a 300 kV microscope (blue) and for a 200 kV microscope (red) when $\Delta\chi(\mathbf{R}) = \pi/2$.

reason stated above. Small fluctuations around the ground truth are expected for unbiased estimates of the true local defocus (Sorzano et al., 2021a; Sorzano et al., 2021b), and this is certainly the case in this experiment (see Fig. 8). Suppose we want to gain accuracy in this step. In that case, we may take an average (or median) of the different estimates, and the average should have less noise than any of the individual estimations. Fig. 9 shows the Median Absolute Dispersion (MAD) between the estimations of the local defocus for each particle. It can be observed that most of the local defocus estimates are within 50Å. A defocus error of 50Å means a shift of $\pi/2$ in the CTF at a resolution of 1.4Å, which will cause a wrong correction of the CTF, which will worsen the final resolution (see Supplementary material Fig. S-2). Logically, the accuracy in the estimation of the local defocus is directly related to the achievable resolution in the reconstructed map (Zhang and Zhou, 2011). This is shown in Fig. 10, which has been generated from Eq. 2(Sorzano et al., 2007),

$$\begin{aligned}\chi(\mathbf{R}) &= \pi\lambda\left(|\Delta f\left(\mathbf{R}\right)||\mathbf{R}|^2 + \frac{1}{2}C_s|\mathbf{R}|^4\lambda^2\right)\\ \Delta\chi(\mathbf{R}) &= \pi\lambda\Delta|\Delta f\left(\mathbf{R}\right)||\mathbf{R}|^2\end{aligned} \tag{2}$$

where C_s represents the spherical aberration coefficient and λ is the electron wavelength computed as:

$$\lambda = \frac{1.23\times10^{-9}}{\sqrt{V + 10^{-6}V^2}}, \tag{3}$$

V is the acceleration voltage of the microscope. The MAD of the different local defocus estimates can be used to filter out those particles whose defocus is uncertain.

Finally, we have performed a reconstruction for each local defocus estimation keeping the same alignment (angles and shifts) in all the cases, which are shown in Fig. 11 showing the local resolution (local resolution histograms are in Supplementary material Fig. S-3) and the corresponding Fourier Shell Correlation (FSC, computed in Xmipp) in Fig. 12. Note that for this specific dataset the only local defocus estimation that has improved the global resolution is the one computed by CryoSPARC, which has obtained an improvement in global resolution of 0.1Å(from 2.1Åto 2.0Å). A similar result has been obtained with EMPIAR 10647 dataset (a non-globular protein), shown in Figs. S-4 and S-5 of Supplementary materials.

3.3. Local defocus refinement is not always helpful

In this section, we show the global and local defocus estimations for beta-galactosidase (EMPIAR 10061). As shown in Fig. 13 (local resolution histograms are shown in the Supplementary material Fig. S-6). In this case, local defocus estimations worsen the resolution achieved in the reconstruction, except for Gctf estimation, which remains similar to global defocus estimation. Thus, in this case, it seems that is not worth refining local defocus estimation. The cause is unknown, but for some reason, the local refinement programs cannot correctly estimate the local defocus.

4. Conclusions

To achieve the highest possible resolution in Cryo-EM SPA, it is important to be precise when estimating every parameter. Thus,

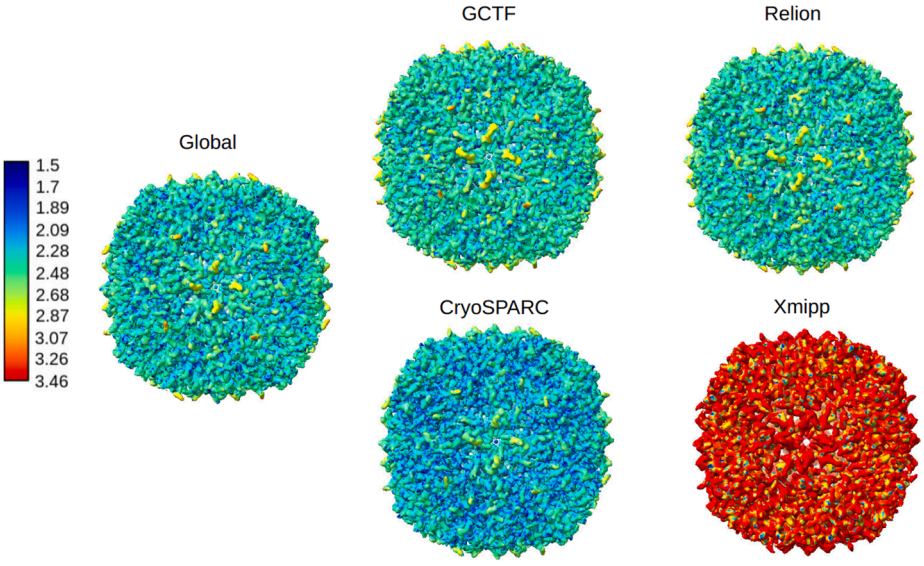

Fig. 11. Local resolution computed with Monores(Vilas et al., 2018) of reconstructed density maps with global defocus and local defocus computed by the existent state-of-the-art methods, keeping the same alignment (angles and shifts) in all the cases.

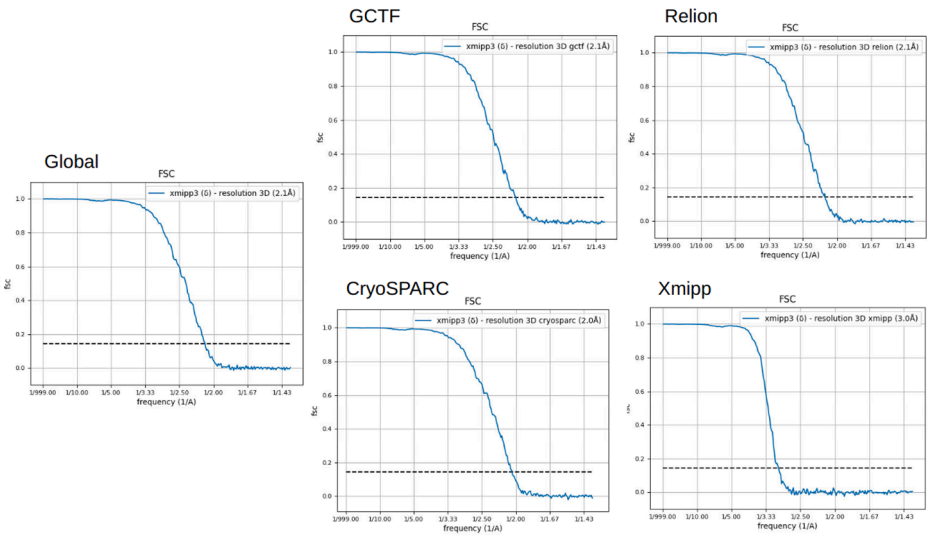

Fig. 12. Fourier Shell Correlation (FCS) to measure the global resolution of each apoferritin reconstruction in Fig. 11.

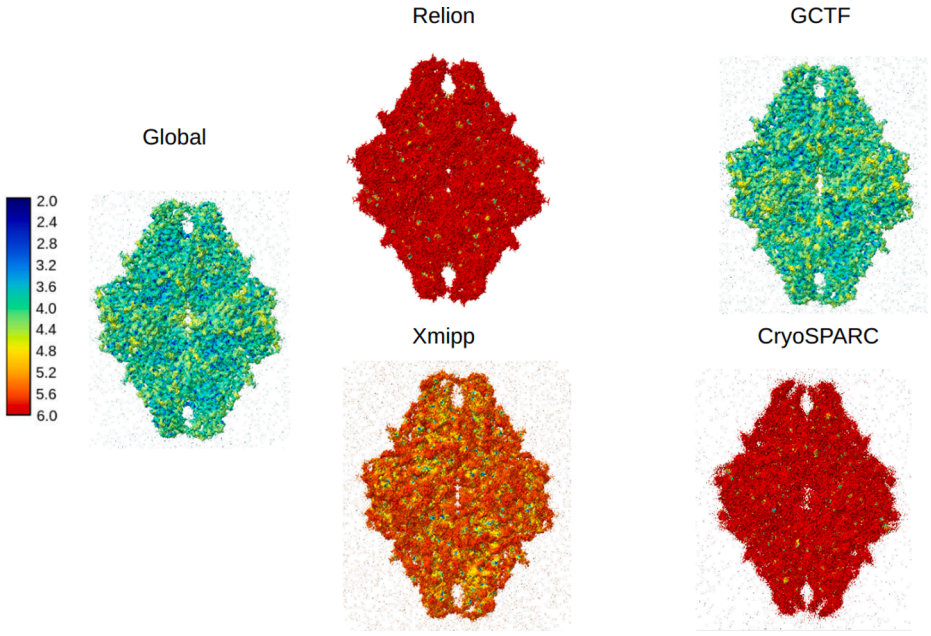

Fig. 13. Local resolution of refined density maps with global defocus and the different local defocus computed by the existent state-of-the-art methods.

estimating an accurate defocus for each particle instead of just a global value per micrograph should result in a more reliable reconstructed map. A global defocus per micrograph assumes that all particles within the micrograph are at the same height (same defocus) with respect to the imaging plane. But we know that it is not true. If these differences in defocus in the same micrograph are not properly corrected, these inaccuracies will lead to blurring and to an inaccurate CTF correction when refining the volume. These factors are limiting as a high resolution is approached (Zhang and Zhou, 2011).

In this work, we have tried four different state-of-the-art programs (Gctf, Relion, CryoSPARC, and Xmipp) to compute local defocus. Their estimations are close, although a deeper analysis reveals noticeable differences, especially because refinement is a step performed to gain accuracy. As with many other parameters in SPA, we cannot know the ground truth for the local defocus of each particle, and thus, we cannot know which estimation (if any) is correct. Then, the best we can do to evaluate our estimations before computing the reconstructions, in order to help with the interpretation of local CTF estimations (not the CTF estimation itself) potentially in those datasets that show large CTF variations, is to compare the estimations computed by the different defocus refinement methods. To do so, we have developed an analysis protocol inside Scipion that allows us to study in detail the resulting defocus estimation of the different programs and put them in the same framework to compare them directly.

Moreover, we have checked that none of the estimations produces unreasonable results that would immediately suggest discarding them. However, the results produced by different programs do not show a clear consensus using the current test datasets.

We recall that it is known that relatively small errors in defocus (50–100Å) translate into noticeable offsets ($\pi/2$) in CTF at high resolution (1.4–2Å), which are indeed resolution values reported in resolved structures nowadays. This fact indicates that the type of defoci differences between methods that we are reporting in this work may be a limiting factor when working at very high-resolution regimes.

Local CTF estimation remains a complex issue and, as a final note, we remark that local defocus refinement does not result always in an

improvement, especially when the signal-to-noise ratio (SNR) is low and the resolution achieved is not good and homogeneous, as we show with the beta-galactosidase example.

Declaration of Competing Interest

The authors declare that they have no known competing financial interests or personal relationships that could have appeared to influence the work reported in this paper.

Data availability

No data was used for the research described in the article.

Acknowledgements

We thank the Spanish National Center for Biotechnology Cryo-EM Facility for yielding the data for this study, especially Javier Chichón and Roberto Melero from I2PC. The authors acknowledge also the economic support from MICIN through grant PID2019 - 104757RB - I00 funded by MCIN/ AEI/ 10.13039/ 501100011033/ and "ERDF A way of making Europe", by the "European Union". To the European Union (EU) and Horizon 2020 through grant: HighResCells (ERC - 2018 - SyG, Proposal: 810057).

Appendix A. Supplementary material

Supplementary data associated with this article can be found, in the online version, at https://doi.org/10.1016/j.jsb.2023.108030.

References

Danev, R., et al., 2020. Fast and accurate defocus modulation for improved tunability of cryo-EM experiments. IUCrJ 7 (3), 566–574.
de la Rosa-Trevin, J.M., et al., 2016. Scipion: A software framework toward integration, reproducibility and validation in 3D electron microscopy. J. Struct. Biol. 195, 93–99.
de la Rosa-Trevin J.M., et al. Xmipp 3.0: An improved software suite for image processing in electron microscopy. In: Journal of Structural Biology 184.2 (2013), pp. 321–328. doi: 10.1016/j.jsb.2013.09.015.
Jimenez-Moreno, A., et al., 2021. Cryo-EM and Single-Particle Analysis with Scipion. J. Visual. Exp.: JoVE.
Neumann, P., Dickmanns, A., Ficner, R., 2018. Validating resolution revolution. Structure 785–795.
Noble, A.J., et al., 2018. Routine single particle cryoEM sample and grid characterization by tomography. eLife.
Punjani, A., Fleet, D.J., 2020. 3D variability analysis: directly resolving continuous flexibility and discrete heterogeneity from single particle cryo-EM images. bioRxiv. https://doi.org/10.1101/2020.04.08.032466.
Punjani, A., et al., 2017. cryoSPARC: algorithms for rapid unsupervised cryo-EM structure determination. Nat. Methods 14, 290–296.
Sorzano, C.O.S., et al., 2018. A new algorithm for high-resolution reconstruction of single particles by electron microscopy. J. Struct. Biol. 204, 329–337.
Sorzano, C.O.S., et al., 2007. Fast, robust and accurate determination of transmission electron microscopy contrast transfer function. J. Struct. Biol. 160, 249–262.
Sorzano C.O.S. et al., 2021a. Image Processing in Cryo-Electron Microscopy of Single Particles: The Power of Combining Methods. In: Structural Proteomics (2021), pp. 257–289.
Sorzano, C.O.S., et al., 2021b. On bias, variance, overfitting, gold standard and consensus in single-particle analysis by cryo-electron microscopy. Acta Crystallogr. Sect. D 78, 410–423.
Sorzano, C.O.S., et al., 2004. XMIPP: A new generation of an open-source image processing package for Electron Microscopy. J. Struct. Biol. 148, 194–204.
Strelak, D., et al., 2021. Advances in Xmipp for Cryo-Electron Microscopy: From Xmipp to Scipion. Molecules 26, 20.
Vilas, J.L., et al., 2018. MonoRes: automatic and unbiased estimation of Local Resolution for electron microscopy Maps. Structure 26, 337–344.
Vilas, J.L., Carazo, J.M., Sorzano, C.O.S., 2022. Emerging themes in CryoEM-single particle analysis image processing. Chem. Rev. 122 (17), 13915–13951.
Wagner, T., et al., 2019. SPHIRE-crYOLO is a fast and accurate fully automated particle picker for cryo-EM. In: Communications Biology 2, p. 218.
Yip, K.M., et al., 2020. Atomic-resolution protein structure determination by Cryo-EM. Nature 587, 157–161.
Zhang, K., 2016. Gctf: real-time CTF determination and correction. J. Struct. Biol. 193, 1–12.
Zhang, X., Zhou, Z.H., 2011. Limiting factors in atomic resolution cryo electron microscopy: no simple tricks. J. Struct. Biol. 175, 253–263.
Zheng, S.Q., et al., 2017. MotionCor2: anisotropic correction of beam-induced motion for improved cryo-electron microscopy. Nat. Methods 14, 331–332.
Zivanov, J., Nakane, T., Scheres, S.H.W., 2020. Estimation of high-order aberrations and anisotropic magnification from cryo-EM data sets in Relion-3.1. IUCrJ 7, 253–267.

Supplementary material

Estrella Fernandez-Gimenez[1,2], J.M. Carazo[1], and C.O.S. Sorzano[1,*]

[1]Centro Nac. Biotecnologia (CSIC), c/Darwin, 3, 28049 Cantoblanco, Madrid, Spain
[2]Univ. Autonoma de Madrid, 28049 Cantoblanco, Madrid, Spain
[*]Corresponding author at: Centro Nac. Biotecnologia (CSIC), c/Darwin, 3, 28049 Cantoblanco, Madrid, Spain. E-mail address: coss@cnb.csic.es (C.O.S. Sorzano).

July 2023

1 Apoferritin

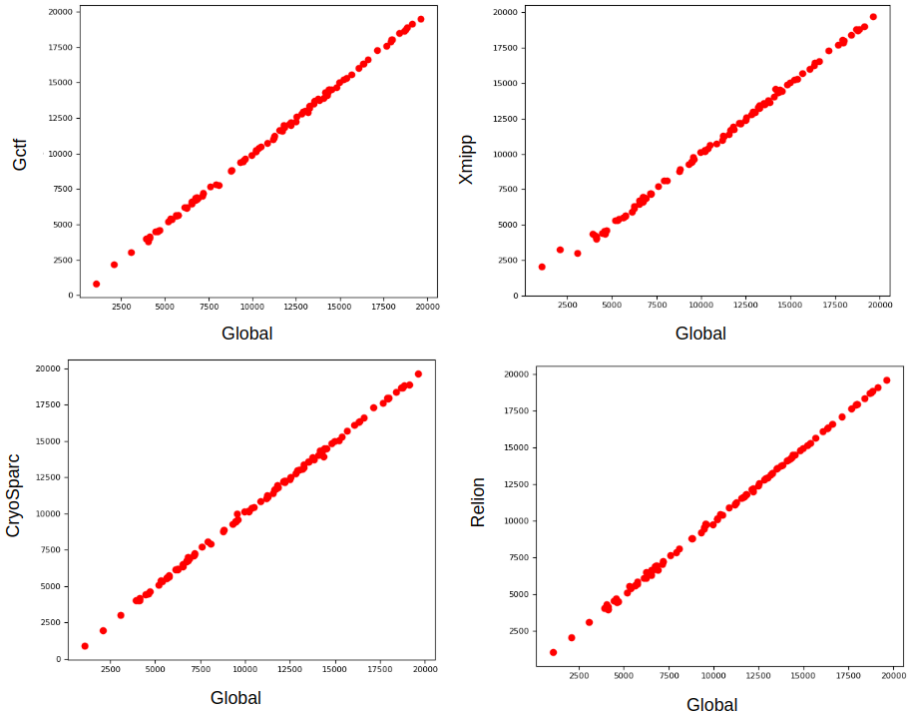

Figure S-1: Scatter plots comparing the local defoci estimations of each method versus the global defoci estimation for a set of random particles of the data set (from micrographs with different defoci) to see how they correlate.

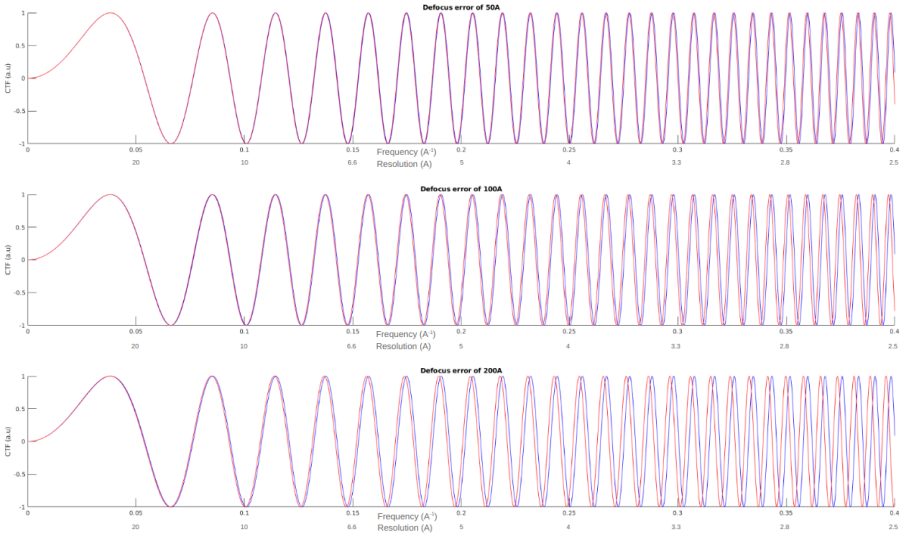

Figure S-2: Offset in CTF produced by different defocus errors. An offset of $\Delta\chi(\mathbf{R}) = \pi/2$ with a defocus error of 50Å occurs approximately at 1.4Å resolution. With a defocus error of 100Å, it occurs at 2Å and with a defocus error of 200Å occurs at 3.3Å, which are all resolutions achievable nowadays.

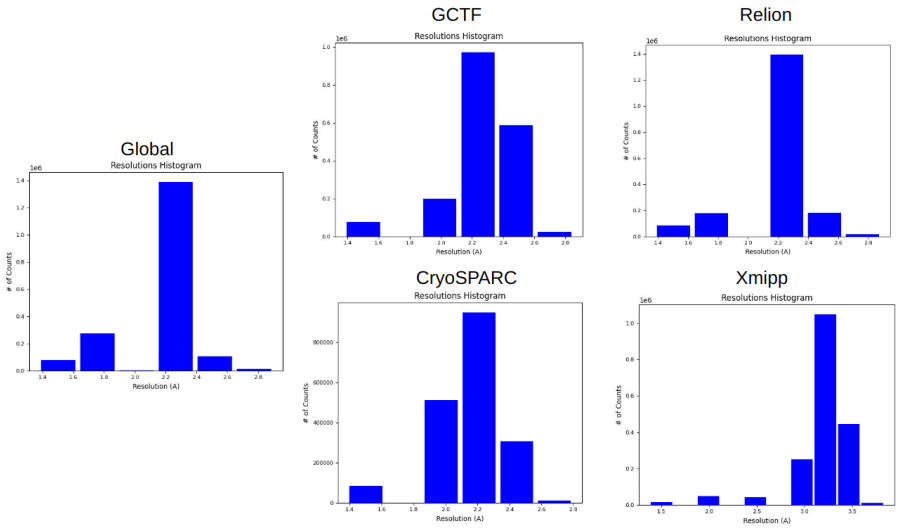

Figure S-3: Resolution histograms of apoferritin with different defocus. The histograms have been computed with MonoRes.

2 PKM2 Enzyme (EMPIAR 10647)

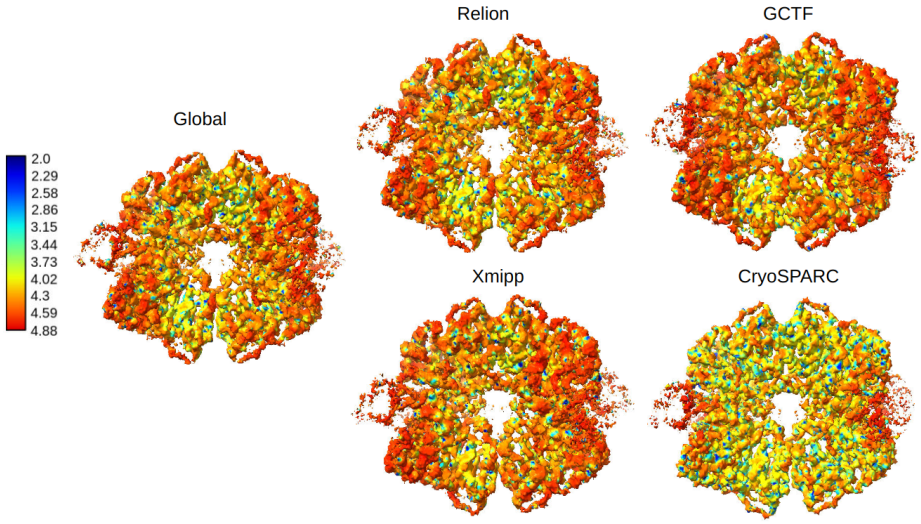

Figure S-4: Local resolution of refined density maps with global defocus and local defocus computed by the existent state-of-the-art methods.

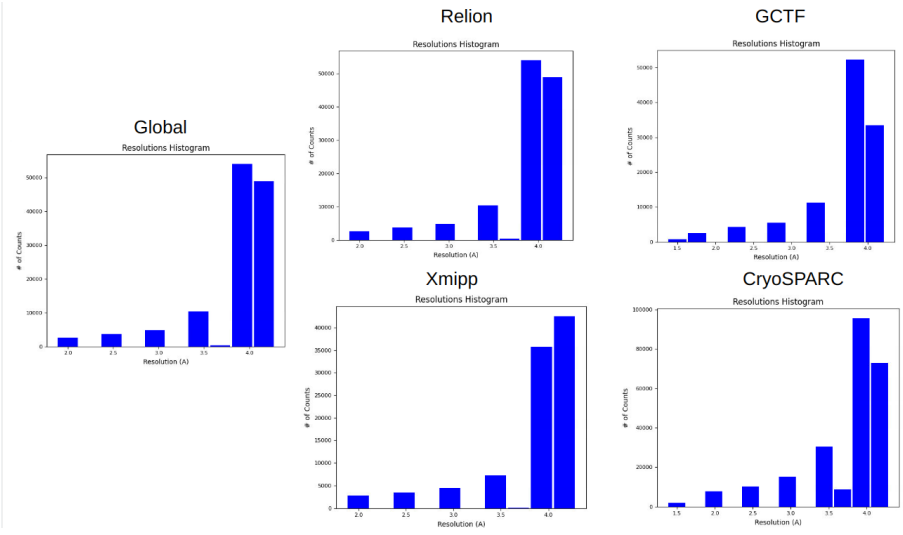

Figure S-5: Resolution histograms of PKM2 enzyme with different defocus. The histograms have been computed with MonoRes.

3 Beta-galactosidase (EMPIAR 10061)

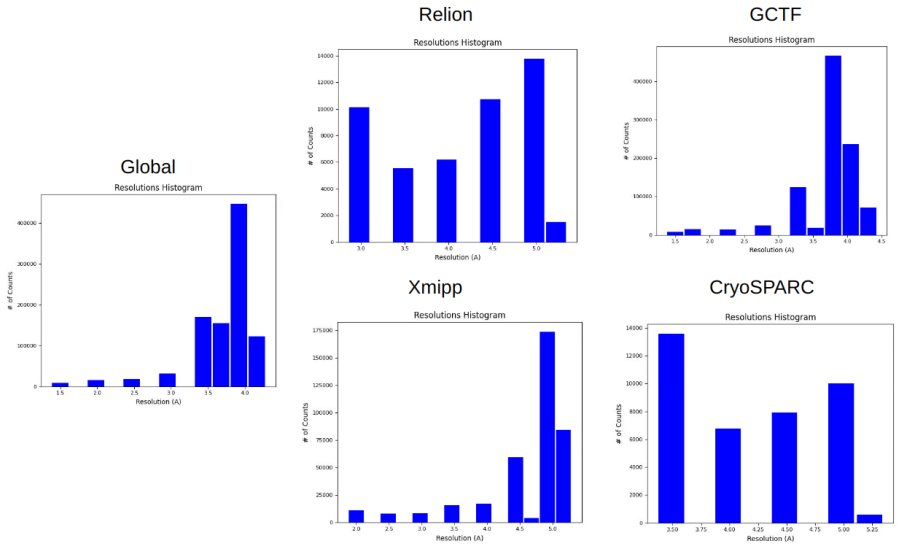

Figure S-6: Resolution histograms of beta-galactosidase with different defocus. The histograms have been computed with MonoRes.